AIAA JOURNAL
Vol. 32, No. 8, August 1994

Technical Notes

TECHNICAL NOTES are short manuscripts describing new developments or important results of a preliminary nature. These Notes cannot exceed 6 manuscript pages and 3 figures; a page of text may be substituted for a figure and vice versa. After informal review by the editors, they may be published within a few months of the date of receipt. Style requirements are the same as for regular contributions (see inside back cover).

High-Resolution Navier-Stokes Computation of Vortical Flow over a Supersonic Delta Wing

C. H. Tai,* C. Y. Soong,† and S. L. Yin‡
Chung Cheng Institute of Technology,
Tahsi, Taoyuan, Taiwan 33509, Republic of China

Introduction

VORTEX flow associated with flow separation from a sharp leading edge plays an important role in the aerodynamic performance of aircraft at high incidence. For better understanding of the detailed flow structure on the leeside of a delta wing, local flow visualization, either experimental or numerical, is required. Flow visualization in supersonic wind tunnels contributes merely in a two-dimensional sense, and some details of the local flow may be overlooked. Comparatively, a high-resolution computational fluid dynamics solution may provide an opportunity to visualize the detailed three-dimensional flows. Viscous effect is closely related to some key phenomena in this vortical flow and, therefore, should be considered. In the solution of the viscous flows, usually, the conical flow approximation is invoked to reduce the computational efforts. However, the flowfield may not be strictly conical over the whole wing. In the present work, Roe's upwind scheme[1] and the modified Baldwin-Lomax model[2] are used in the computations of the supersonic flow at $M_\infty = 2.8$ and $Re = 2.2 \times 10^6$ around a 75-deg swept delta wing at 16-deg angle of attack. The flowfield is a typical case of the classical vortex with shock in the α_n-M_n parameter map.[3] To examine the upstream effect of the wake flow in the base region of a finite wing, a multiblock strategy is employed. Details of the vortical flow structure and its sensitivity to the grid system and numerical scheme employed are investigated. Furthermore, the appropriateness of the conical approximation and the wake upstream effect are addressed.

Methodology

Reynolds-averaged equations in conservative form are considered. The spatial discretization is performed by using Roe's flux difference splitting scheme. The explicit Runge-Kutta method is employed to integrate the pseudounsteady equations to achieve the steady-state solutions. In the computations, the van Leer κ-scheme[4] and the van Albada limiter[5] are implemented. To insure a smooth transition from subsonic to supersonic flows, a proper entropy correction[6] is used. The solution procedure is terminated as the residual reduces to the value less than 10^{-5}.

The computational domain is a frustum of a half-hemispherical cylinder with a radius of $3C$ (C = root chord of the wing). An H-O type grid is generated at each axial station by the two-dimensional hyperbolic grid generation developed by the present authors.[7] The apex and trailing-edge grids are duplicated for the upstream and downstream regions of the wing, respectively. A grid block for the base region is inserted into the main grid for multiblock computations.

Results and Discussion

Results of the numerical experiments on the solution sensitivity to the grid arrangement and the numerical scheme are shown in Fig. 1a. The details of the test cases are listed in Table 1.

As shown in Fig. 1a, the C_p distributions by high-order scheme (i.e., $\kappa = 1/3$ in the κ-scheme) are fairly good for the various grids. It is observed that the results on the multiblock (MB) grid $56 \times 75 \times 48$ with the first grid spacing $\Delta S/Y_{LE} = 5 \times 10^{-4}$ over the surface agree very well with the experimental data.[3] It is also noticed that, even on a relatively finer grid, the first-order scheme still fails to generate a satisfactory result. As the first grid spacing becomes large, e.g., $\Delta S/Y_{LE} = 1 \times 10^{-3}$, the solutions seem to devi-

Table 1 Test cases for the solution sensitivity to the numerical procedure

	Case A	Case B	Case C	Case D
Grid no.	$96 \times 65 \times 48$	$56 \times 75 \times 64$	$56 \times 75 \times 64$	$56 \times 75 \times 48$ MB
$\Delta S/Y_{LE}$	5×10^{-4}	1×10^{-3}	5×10^{-4}	5×10^{-4}
Scheme	High order	High order	First order	High order

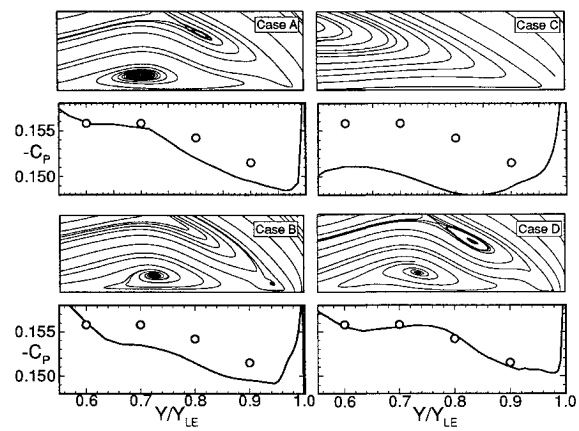

Fig. 1a Solution sensitivity to the numerical procedures.

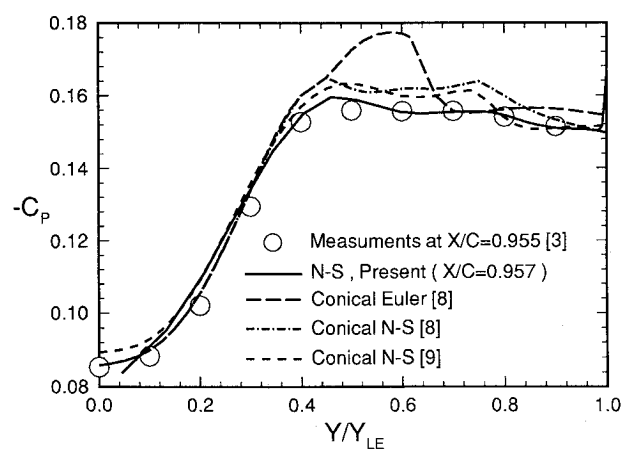

Fig. 1b Comparison of the computational results with the measurements.

Received July 17, 1993; revision received Jan. 7, 1994; accepted for publication Jan. 14, 1994.

*Associate Professor, Department of Mechanical Engineering.
†Associate Professor, Department of Aeronautical Engineering. Member AIAA.
‡Ph.D. Candidate, Department of Systems Engineering.

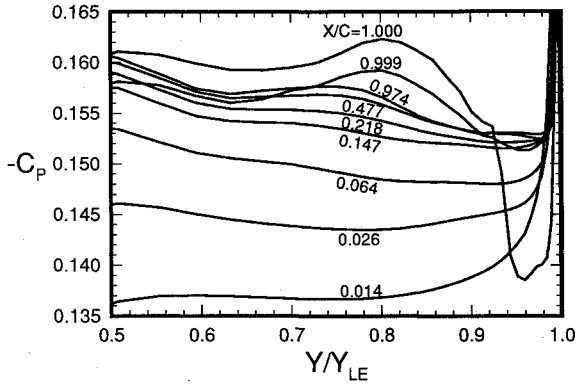

Fig. 2 Spanwise pressure distributions at various axial stations.

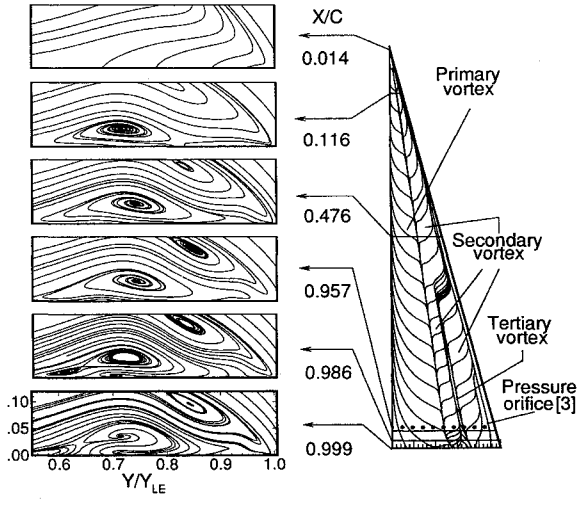

Fig. 3 Crossflow and surface streamline patterns at various axial stations.

ate from the measurements for the worse resolution in the boundary-layer region. In the close-up view shown in Fig. 1a, it is observed that the crossflow maps are highly dependent on the grid and scheme used in the computations. It is believed that the crossflow structure characterized by the presence of the primary, secondary, and tertiary vortices in case D is more convincing. Figure 1b shows the comparisons of the present multiblock/high-order solution with the measurements,[3] Euler,[8] and conical Navier-Stokes[8,9] solutions. Obviously, in consideration of the wing thickness as well as the wake flow, the present two-block strategy is more appropriate than the single block arrangement.

Figure 2 reveals that the C_p curves are very different in the apex and trailing regions, whereas in the middle portion of the wing (see the curves for $X/C=0.477$ and 0.974), the pressure distribution appears nearly invariant in longitudinal direction. By examining the crossflow and the surface streamline patterns in Fig. 3, it is noted that the vortical flow is developing from the apex to the midwing location, say $X/C=0.48$. In the successive portion, i.e., $0.48<X/C<0.95$, the global flow structure can be regarded as developed and conical in nature, whereas the tertiary vortex emerges at $X/C>0.6$. Fortunately, this weak vortex does not affect C_p significantly. In the trailing portion of the wing, the flow becomes more complicated due to the upstream effect of the wake flow in base region. Although the flow is supersonic, the presence of the base flow and its influence can propagate upstream through the subsonic region in the boundary layer and alter the flow in the trailing region of $X/C>0.95$.

Figure 4 gives a clear view of particle path trajectories, in which fluid flow in the wake and wing trailing regions are also presented. To emphasize the upstream effect of the wake flow and make a visible and clear picture, the wake fluid particle paths are cut off as appropriate. It is observed in Fig. 4 that some of the

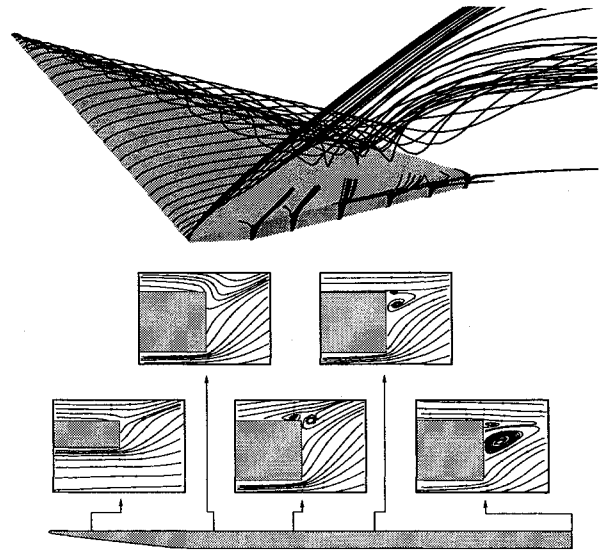

Fig. 4 Particle path trajectories and details of base flow patterns.

wake fluid particles coming from the windward side move downstream toward the far field, but the others migrate upstream and therefore alter the leeward flow in the trailing region of the wing. The transverse particle paths in the inboard part of the base region represent small vortices as those shown in the close-up views in Fig. 4.

Concluding Remarks

The viscous vortical flows near the leading edge of a delta wing are very sensitive to the numerical procedure. Different arrangement of the grid and/or the scheme employed may result in distinct vortex solutions. For an accurate prediction of the detailed flow structure with the presence of the wake effect, a high-order scheme and a multiblock grid system with appropriate resolution are necessary.

Conical flow assumption is valid in the middle portion of the wing but is not a good approximation for the upstream part of the wing for the developing nature of the vortical flow. With the presence of the base flow in the present case of a finite-thickness-finite-chord wing, the upstream effect of the wake breaks down the conical similarity in the trailing region of the wing. This upstream effect cannot be predicted in the case of infinite-chord and/or zero-thickness models, and it is also a drawback of the thin-layer computations.

Acknowledgment

This research was supported in part by the National Science Council of the Republic of China under Grant NSC 82-0401-E-014-005.

References

[1]Roe, P. L., "Approximate Riemann Solvers Parameter Vectors and Difference Scheme," *Journal of Computational Physics*, Vol. 43, No. 2, 1981, pp. 357–372.

[2]Degani, D., and Schiff, L. B., "Computation of Supersonic Viscous Flows Around Pointed Bodies at Large Incidence," AIAA Paper 83-0034, Jan. 1983.

[3] Miller, D. S., and Wood, R. M., "Lee-Side Flow over Delta Wings at Supersonic Speeds," NASA TP-2430, June 1985.

[4]van Leer, B., "Upwind-Difference Methods for Aerodynamic Problems Governed by the Euler Equations, in Large-Scale Computations in Fluid Mechanics," *Lectures in Applied Mathematics*, edited by B. E. Engquist, S. Osher, and R. C. J. Somerville, Vol. 22, American Mathematical Society, Providence, RI, 1985, pp. 327–336.

[5]van Albada, D., van Leer, B., and Roberts, W. W., "A Comparative Study of Computational Methods in Cosmic Gas Dynamics," *Astronomy and Astrophysics*, Vol. 108, 1982, pp. 76–84.

[6]van Leer, B., Lee, W. T., and Powell, K. G., "Sonic-Point Capturing,"

AIAA Paper 89-1945, June 1989.

[7]Tai, C. H., Yin, S. L., and Soong, C. Y., "A Novel Hyperbolic Grid Generation Procedure with Inherent Adaptive Dissipation," *Journal of Computational Physics* (submitted for publication).

[8]McMillin, S. N., Thomas, J. L., and Murman, E. M.,"Navier-Stokes and Euler Solutions for the Lee-Side Flows over Supersonic Delta Wings," NASA TP-3035, Dec. 1990.

[9]Obayashi, S., and Goorjian, P. M., "Improvements and Applications of a Streamwise Upwind Algorithm," AIAA Paper 89-1957, June 1989.

Unstructured Viscous Grid Generation by the Advancing-Layers Method

Shahyar Pirzadeh*
ViGYAN, Inc., Hampton, Virginia 23666

Introduction

DURING the past few years, computational fluid dynamics has progressed to the point that routine, accurate inviscid-flow computations are now possible for practical, realistic configurations in short periods of time. A significant contribution to the recent accomplishment has been due to the emergence of new, efficient grid generation techniques. Unstructured grids, for example, have been extremely successful in simplifying the discretization of complex computational domains for inviscid-flow computations. However, the generation of unstructured grids for routine computation of the Navier-Stokes equations remains a challenging task. Unlike the variety of the Euler grid generation techniques available, there are only a few methods in the literature addressing the problem of viscous, unstructured or hybrid structured/unstructured grid generation. Among these are the methods reported in Refs. 1–4. Relying on the conventional structured grid techniques, some of the existing methods retain the limitations of structured grids and, thus, may lack the required flexibility and robustness for handling complex configurations.

This paper introduces an alternate approach for generating highly stretched unstructured triangular grids. The method is entirely based on an advancing-front technique and, thus, benefits from the flexibility and grid quality of the conventional advancing-front-based Euler grid generators. In this Note, the basic concept of the methodology and some preliminary results in two dimensions are presented.

Approach

The proposed grid generation process is divided into three separate stages: 1) surface grid generation, 2) construction of high-aspect-ratio cells in the viscous-dominated flow region, and 3) generation of a regular (isotropic) grid outside the boundary layer. An existing robust advancing-front-based Euler grid generation system (VGRID)[5,6] is used to perform steps 1 and 3.

Because of the high-aspect-ratio requirement for cells in the boundary layer, a regular advancing-front strategy, like that conventionally used for Euler grid generation, is inadequate for the generation of highly stretched grids without extensive modifications. Such enhancement would require an automatic distribution of grid points densely in one direction and sparsely in other(s) in the boundary layer, and isotropic point distribution elsewhere. This, in turn, would require additional information regarding a variant, multidirectional grid stretching prescribed in the field and a sophisticated mechanism for smooth distribution of stretching data and coordinate transformations. All of these additional elements would adversely affect the entire process of the conventional advancing front for constructing cells of high (several orders of magnitude) aspect ratio and extremely small spacing.

The process of viscous grid generation is greatly simplified if the construction of high-aspect-ratio cells in the boundary layer is performed separately from that of regular unstretched cells outside the viscous-flow region. To that end, a special advancing-front strategy, referred to here as "advancing layers," has been devised for specific generation of stretched cells (step 2). The goal is to maintain the desirable features of the original advancing-front method, i.e., high degree of flexibility, robustness, and good grid quality. The new method is compatible with and supplemental to the conventional advancing-front technique. Although the overall procedure employs two different techniques in separate stages, the entire process is performed continuously with an automatic switch from one method to another.

As in the conventional advancing-front technique, grid cells begin forming individually from the boundaries and march into the domain. However, unlike the generation procedure of the conventional method in which cells are added in no systematic sequence, the construction of a stretched grid is performed by advancing one layer of cells at a time. This strategy is employed to 1) minimize the front congestion, 2) minimize the complexity of search-and-check operations when forming a cell, and 3) evenly distribute stretched cells on all solid boundaries as much as possible. By bringing this order into the advancing-front process, not only does the operation become less complicated, but its efficiency also improves considerably.

Because of the concentration of grid points over a small length scale across the boundary layer, the position of each new point being introduced in the field has a significant effect on the quality of the generated viscous grid. Likewise, the complexity of the grid marching process largely depends on the arrangement of grid points in the boundary layer, especially at sharp corners. To ensure a good grid quality and to facilitate the process, new grid points are positioned along a set of predetermined vectors. The vectors are determined once at each surface mesh point by simply averaging the normal vectors of the faces sharing the point and then smoothing the vectors by a Laplacian smoothing operation. Although this simple procedure is sufficient for calculating the surface vectors in two dimensions, it requires further treatment for three-dimensional problems to prevent the formation of overlapped cells at sharp convex corners.

The advancing-layers process proceeds by successively selecting faces from a list of active faces on the front and connecting them to the new points inserted along the corresponding surface vectors (Fig. 1). The distribution of grid points along the vectors is determined by a stretching function. This is in contrast to prescribing point distribution from information stored in a background grid as is used in the conventional advancing-front method.[7] After a cell is constructed, the old face becomes inactive and is removed from the front, and new faces are created and added to the list. Three types of faces are identified (see Fig. 1) on the front as the layers advance in the field: 1) faces with both nodes on the same layer (level) referred to as primary faces, 2) faces with their nodes on different levels and along different surface vectors (secondary faces), and 3) faces with nodes on different levels but along the same vector (cross-sectional faces). Only the primary and secondary faces are selected to form cells. Although considered active, a cross-sectional face is simply skipped as it will eventually be removed along with an adjacent primary or secondary face. To form

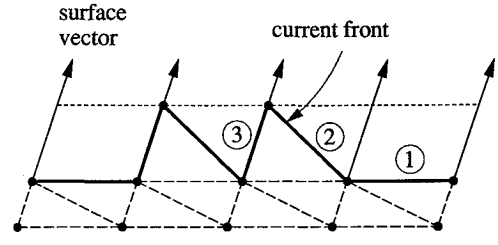

Fig. 1 Layers of triangular cells with different face types on the front: 1) primary face, 2) secondary face, and 3) cross-sectional face.

Received June 8, 1993; presented as Paper 93-3453 at the AIAA 11th Applied Aerodynamics Conference, Monterey, CA, Aug. 9–11, 1993; revision received Feb. 4, 1994; accepted for publication Feb. 7, 1994.

*Senior Research Engineer, 30 Research Drive. Member AIAA.